UDC 550.8+550.84.09

GEOPHYSICAL EXPLORATIONS BY RESISTIVITY AND INDUCED POLARIZATION METHODS FOR THE COPPER DEPOSIT, SOUTH KHORASAN, IRAN

Adel Shirazy[1],
Adel.shirazy@shahroodut.ac.ir

Ardeshir Hezarkhani[1],
Ardehez@aut.ac.ir

Aref Shirazy[1],
Aref.shirazi@aut.ac.ir

Timofey V. Timkin[2],
timkin@tpu.ru

Valery G. Voroshilov[2],
v_g_v@tpu.ru

[1] Amirkabir University of Technology (Tehran Polytechnic),
Khafez avenue, 1591634311, Tehran, Iran.

[2] National Research Tomsk Polytechnic University,
30, Lenin avenue, Tomsk, 634050, Russia.

The relevance. *These are the first geophysics studies in the Mesgaran exploration area. Based on geological studies in the mineral zone, copper mineralization was proven. The mineralization type in this area was identified as Cyprus-type massive sulfide. The complexity of the geological structure determines the need to use geophysical research and forecasting methods for planning mining and drilling operations.*
The main aim *of this study is the application of geophysical methods in the search for mineral deposits and modeling of the geological environment.*
Object: *Mesgaran exploration area, South Khorasan province, Iran.*
Methods. *In order to obtain more subsurface information, geophysical methods IP and Rs were used. Five profiles were designed and implemented for geoelectric surveys. Overall, five profiles (P1 to P5) were read as dipole-dipole arrays with 784 points. The profiles were taken east-west and north-south along parallel to the mineralization zones. The dipole-dipole array is designed with the parameters AB=MN=20 m, jump=20 m and up to 6 jumps for MN.*
Results. *In general, four types of anomalies were identified in these investigations. Which to some extent revealed the association of anomalies with the types of rocks and mineralization of the study area: 1) anomalies with low electrical resistivity, as well as low polarity, often correspond to quaternary alluvial deposits; 2) abnormalities with high electrical resistance, and low polarity, which are consistent with limestone's and are often superficial; 3) anomalies with high polarity and high resistance, which in the south of the profiles form altitude and correspond to the agglomerates; 4) anomalies with high polarity and higher relative resistance are associated with igneous masses, which are often composed of andesitic-basaltic rocks. Based on the position of the identified anomalies in the 5 profiles, the optimal location of the drills was determined.*

Key words:
Resistivity, induce polarization, copper deposit, geophysical model, Mesgaran, Iran.

Introduction

Mineral resources as the first link in the production chain play an undeniable role in the development, growth and prosperity of a country and form the basis of the economy and industry [1–4]. From the beginning of its creation and throughout history, human beings have used minerals according to their needs and knowledge [5–7]. In other words, these minerals form the basis of civilization. Therefore, mineral exploration has special importance as the first step in this cycle [8–12]. Along with the production and advancement of science, technology, and innovations such as remote sensing, GIS, and global positioning systems, traditional methods of mineral exploration have been replaced by new methods [13, 14]. Remote sensing is a technique of collecting information about land surface features without physical contact with them [15]. Remote sensing has great potential for identifying altered areas associated with deposit masses thus it is known as a standard method in the field of mineral exploration and it can help to study geochemical and geophysical explorations [16–20]. It should be noted that any mining and exploration operations may damage the environment or the antiquities and geotourism sites [21, 22]. Therefore, by using the updated methods in exploratory studies and mining activities, in addition to higher productivity and avoiding spending a lot of time and money [19, 23–27], the damage to the environment can be reduced as much as possible. In geoelectric surveying, the response of the subsurface is studied with the help of an electrical transmitter-receiver setup [28]. When sulfide minerals are exposed to water and oxygen, they oxidize to form soluble metals and sulfates. Oxidation products tend to increase acidity in the oxidizing site and in the absence of alkalinity to neutralize the acidity, the pH level can decrease significantly. The increased solubility of metals in

acidic water prevents their precipitation and leads to high concentrations of dissolved metals and salts in acidic water. Eventually, surface water will find its way to where the acid is formed and carry pollutants into groundwater systems and surface water bodies [29]. Electrical resistivity surveys are used routinely in geothermal, mining, coal and groundwater and engineering applications. They are used much less routinely in oil and gas exploration. The induced polarization method was developed for detecting small concentrations of disseminated mineralization in base metal exploration [30].

Rich in mineral resources, the central and eastern part of the province of Khorasan is an important metallogenic region in eastern Iran. In recent years, new copper deposits have been discovered in the area adjacent to the study area at Shadan and the adjacent Maherabad mining area [31–34]. Signs of copper mineralization were found in the region under study, only shallow horizons were explored, so there was a need for deep exploration.

Since different geophysical methods reflect different physical parameters of rocks and ores, several methods are usually used to limit the properties of underground minerals and reduce the amount of solutions. In recent years, integrated geophysical survey methods have played an important role in the exploration of metal ores [35–37].

To determine the presence of ore bodies at depth, confirm whether the ore bodies are continuous or discontinuous, evaluate the thickness of the ore bodies, confirm the results with geological information, detect areas without anomalies and determine the optimal points for drilling, a comprehensive geophysical survey was carried out. They will also be useful for finding similar deposits in the region under study, providing guidance on exploration that combines these geophysical methods.

Data and geological setting of the studied area

Regional Geological Setting

The study area is a part of the Sarbisheh geological map (on a scale of 1:10000000) and the Mesgaran copper deposit is located 29 km south of Sarbishheh city. The UTM geographic position is between 0770500 and 0773000 East (longitude) and 3577500 to 3581500 North (latitudes) (Fig. 1).

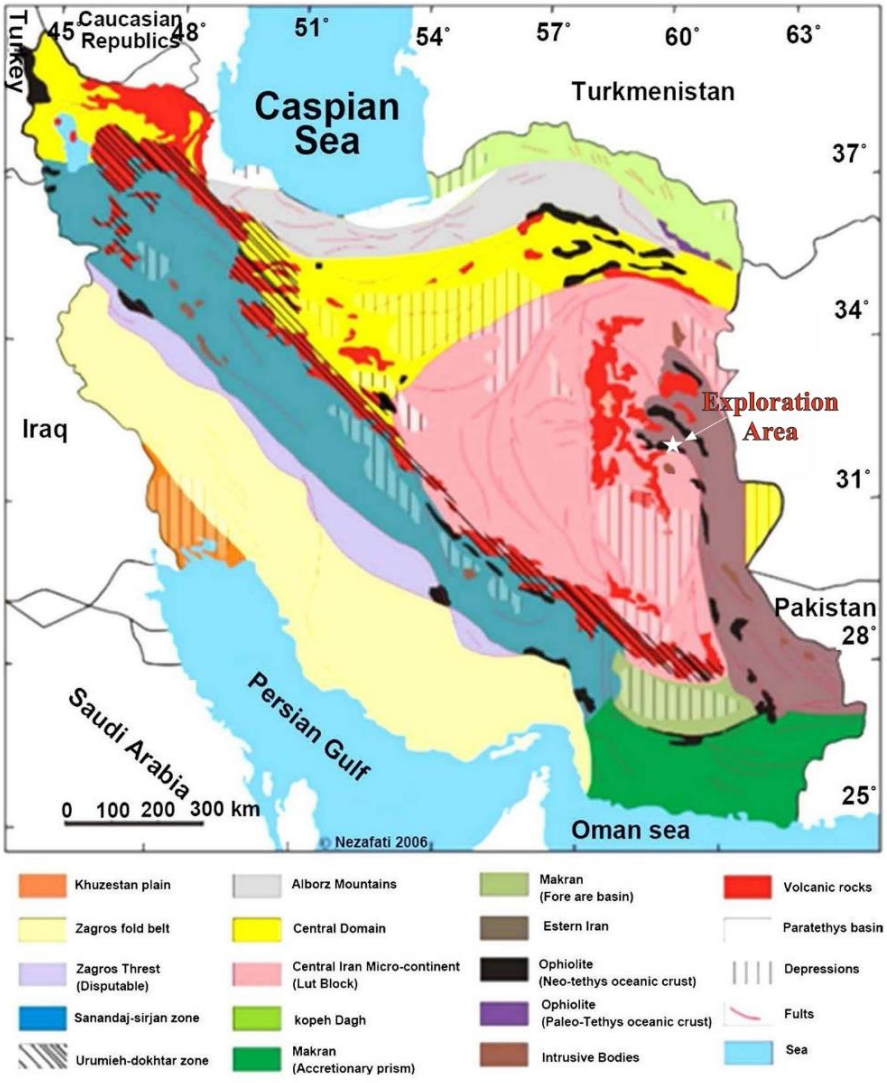

Fig. 1. *Simplified geological map of geographical location of Mesgaran exploration area in west Iran*
Рис. 1. *Схематическая геологическая карта разведочного района Месгаран на западе Ирана*

There are no violent heights in this range, and most of them are dipped and plain. Due to the existence of Mafic and Ultramafic units (ophiolite sequence) and erosion function on these units, the topography of the area is a mild and quiet hill (Fig. 2). The sedimentary sections of the region, in particular, have more rugged topography of limestone than mineral area. In terms of structural and sedimentary divisions, the study area is a small part of the structural zone of the East of Iran and is metallurgically located in the northern part of Ahangaran-Bandaan [38, 39].

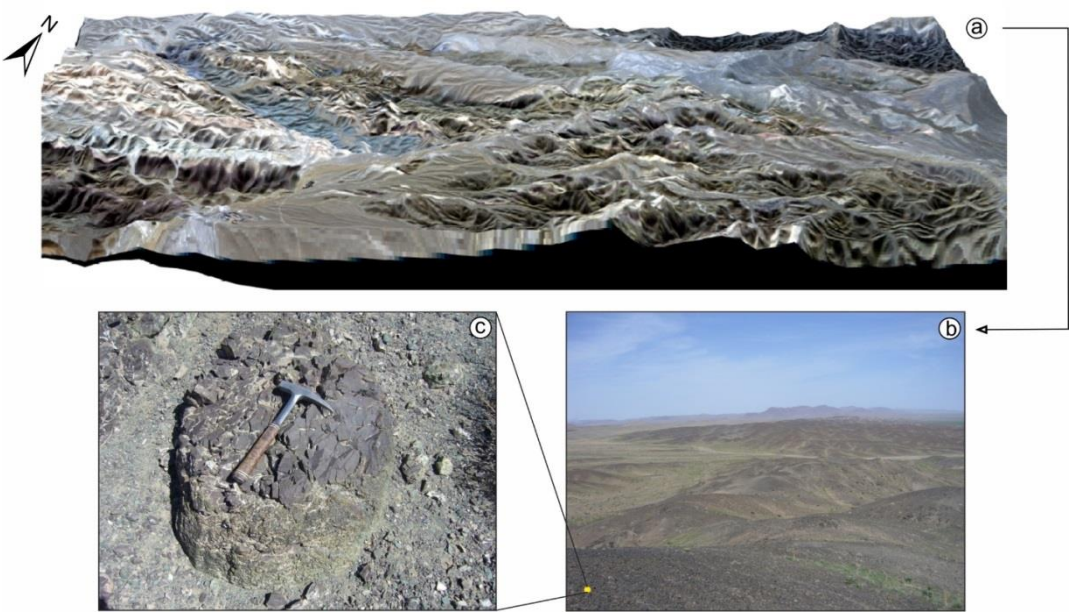

Fig. 2. *(a) Digital elevation models of the Mesgaran exploration area, provided by the QuickBird satellite [11], (b) mild morphology and hills of ultrabasic rocks in the north of Mesraran; (c) view of pillow basalt which outer surface is affected by contact with seawater and cooling and its color and texture have been changed*

Fig. 2. *(a) Цифровая модель рельефа горнорудного района Месгаран (данные со спутника QuickBird) [11], (b) офиолитовые покровы в северной части территории; (c) ксенолит базальта в серпентинитах, внешняя поверхность которого подверглась воздействию контакта с морской водой и охлаждению, что привело к изменению цвет и текстуры*

In terms of lithology, exploratory areas include ultrabasic rocks, dolerite dikes, pillow basalts, calcareous outcrops, phyllite and schist lenses [11, 40] (Fig. 1).

The rock units in the region show a complete ophiolite sequence, but because of the compressive stresses dominant on the region, the boundaries of these units are largely faulty, and the outcrop of ultrabasic rocks, basic rocks and ocean sediments does not follow any order.

Mineralization

In the Mesgaran mining area copper mineralization has occurred in pillow-lava and andesite-basalt sequences of eastern Iran. Two mineralization zones were identified as sulfide mineralization with silicified stockworks (primary mineralization) and supergene mineralization. The primary copper mineralization in this region is mostly in accordance to silicified or carbonate veins with epidote and chlorite in volcanic basalt. These veins cross out the volcanic complex as stockworks which include Chalcopyrite, Bournite and Pyrite. In this region, we observed no evidence proving massive deposit or lens shape deposit creation. The main observed minerals are sulfide and oxide forms of copper. Malachite, azurite and lower amounts of tenorite and native copper in oxide supergene zone and chalcopyrite and bornite as the primary sulfides were detected. Oxidation and erosion caused goethite and hematite around sulfide minerals like chalcopyrite and pyrite. Alteration is observed almost everywhere on the surface but the degree of alteration varies. Generally, alteration occurs when rocks react to hydrothermal and magmatic fluids and this reaction leads to chemical and mineralogic changes. Chlorite alteration occurred on a large scale which is a specific form of propylitic alteration. Al, Fe and Mg-rich fluids cased chlorite alteration in basic rocks [41].

In this region, argillic alteration (presence of montmorillonite mineral) as a secondary alteration is observed as well. Most of the copper is in oxide form on the surface and because of the high degree of oxidation and erosion, sulfide mineralization is rare in outcrops, so rock samples from deep well cores are needed to study the deposit. Drilling is the best choice in such situations. According to mineralization and the host rock (pillow-lava and andesite-basalt), the mineralization type seems to be categorized as a massive sulfide and redbed type. Generally, the mineralization manner (copper mineralization as stockworks), the host rock (pillow-lava and andesite-basalt), the deposit development environment (a volcanic part of an Ophiolite sequence) and the alterations (quartz-carbonate, epidote and chlorite) observed in this region and comparing them to the massive sulfide types leads to classifying Mesgaran deposit as a Volcanic Massive Sulfide (VMS) type. But still more studies are needed to prove this claim with higher accuracy [41].

Methodology and materials

Field operations

In order to study the effect of electrical resistance and IP on the qualitative and quantitative evaluation of copper mineral deposits, the geophysical operations of IP and resistivity with dipole-dipole array were carried out. Overall five profiles (P1 to P5) were read as dipole-dipole arrays with 784 points (Fig. 3). The profiles were taken east-west and north-south along parallel to the mineralization zones.

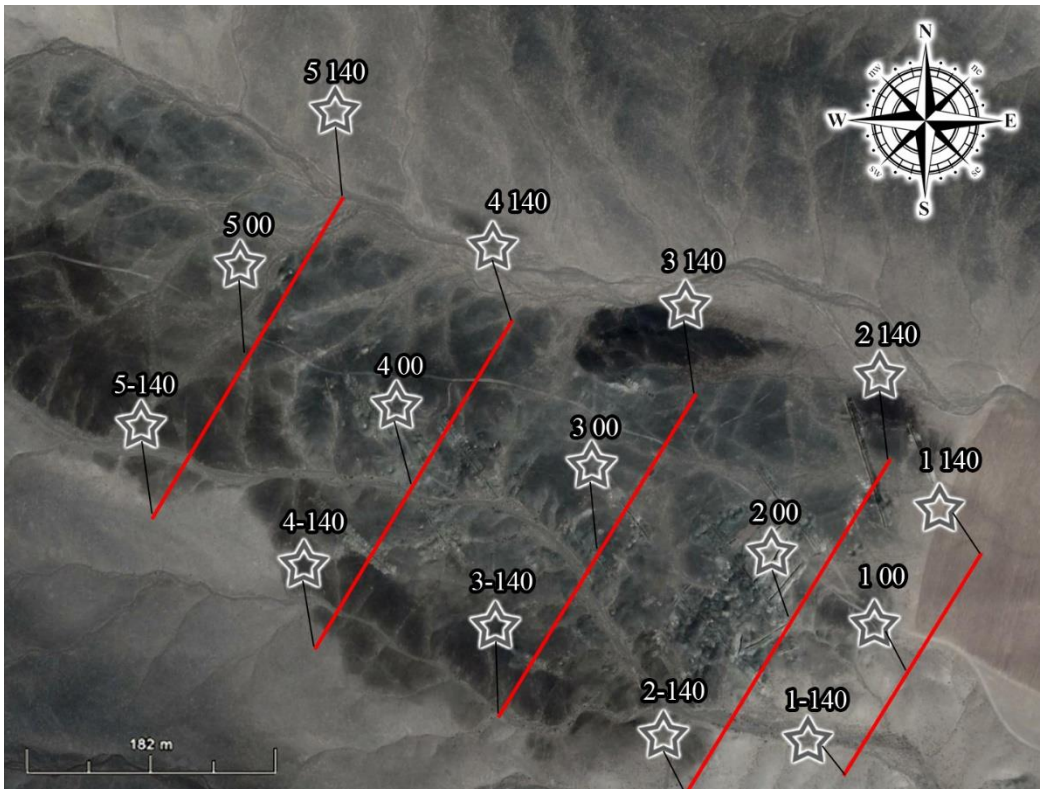

Fig. 3. *Location of geophysical profiles and measurement stations in the exploration area Mesgaran*
Рис. 3. *Расположение геофизических профилей и станций измерения в исследуемом районе Месгаран*

Resistivity geoelectric method

In the resistivity method, the spatial variation of resistivity ρ (or conductivity σ, the inverse) in the field is determined using four-electrode measurements. Two (transmitter) electrodes are deployed to create an electrical circuit. Measurement of the potential difference (voltage) between the two other electrodes permits the determination of apparent resistivity. Inverse methods may be applied to such measurements to determine an image of the subsurface structure, as illustrated later. Electrodes may be placed on the ground surface and/or in boreholes. Stainless steel is the most widely used electrode material for field measurements, although others, such as copper or brass, are also used. To avoid polarization at the electrodes, an alternating power source is utilized. A switched square wave (Fig. 4) is the most common current waveform; it is generally applied at frequencies of about 0,5 to 2 Hz. As it is shown in Fig. 4, a background (self-potential) voltage, V_{sp}, may be observed. Note that the level of this may change over time, but such drift is easily removed owing to the shape of the injected waveform. The measured transfer resistance is given by the equation (1):

$$R=V_p/I_p, \quad (1)$$

where V_p is the primary (peak) voltage and I_p is the injected current, as it is shown in Fig. 5. Note that the voltage series in Fig. 6 is idealized since no capacitive (electrical charge storage) effects are observed [42].

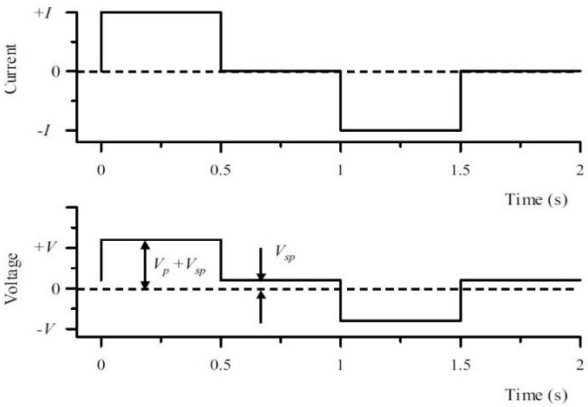

Fig. 4. *Typical current and idealized voltage waveforms for field DC resistivity surveys. V_p is the primary voltage, V_{sp} is the observed self-potential voltage [42]*

Fig. 4. *Типичные формы тока и идеализированного напряжения для полевых исследований удельного сопротивления постоянному току. V_p – первичное напряжение, V_{sp} – наблюдаемое напряжение собственного потенциала [42]*

As it is illustrated in Fig. 5, current flow in homogenous earth from an electrode placed on the ground surface will follow equation (2):

$$V = \frac{\rho I}{2\pi} \frac{1}{r}, \quad (2)$$

where ρ is the resistivity and r the distance from the electrode. Since the apparent resistivity ρ_a is defined as the resistivity of homogenous earth to which the measured transfer resistance is equivalent, this equation may be used with the superposition principle to derive expressions for the apparent resistivity of specific electrode arrangements [43].

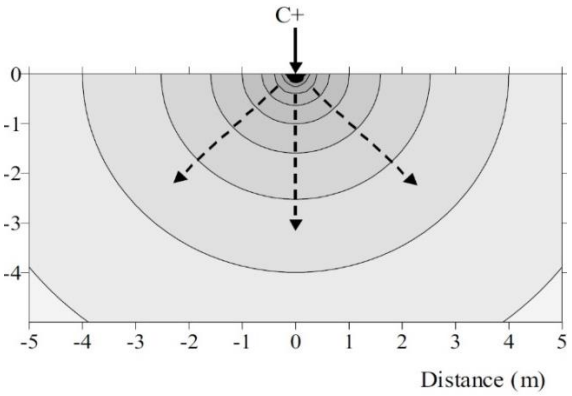

Fig. 5. *Potential variation in a half-space with uniform resistivity distribution due to current injection at the ground surface [42]*

Fig. 5. *Потенциальное изменение в полупространстве с однородным распределением удельного сопротивления из-за подачи тока на поверхность Земли [42]*

A number of electrode configurations are commonly used for ground-surface surveys. Fig. 6 illustrates the Wenner, dipole-dipole, and Schlumberger surveys.

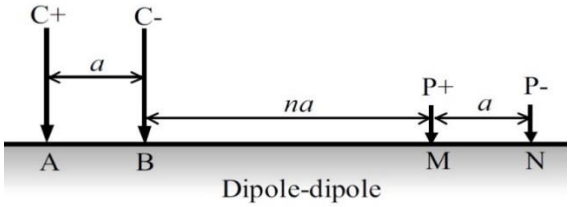

Fig. 6. *Dipole-dipole electrode array [42]*

Fig. 6. *Диполь-дипольная электродная решетка [42]*

Induced Polarization (IP) Geoelectric Method

Induced polarization (IP) methods measure the rates with which electrical charges build up in the ground due to the applied voltage, and at which they balance out after such voltages are removed. Common sources of the effect are charge polarization on individual grains, charge build up within clay layers, and electrochemical interactions at grain surfaces [43]. As the IP effect results from currents passing through the ground, IP surveys always measure resistivity in addition to some index of polarization. The reported polarization index is different for different IP equipment; it may be changeability in mV-sec/V, percent frequency effect (a dimensionless percentage), or phase shift in milliradians between transmitted and received signals [44]. While soil resistivity is controlled primarily by electrical conductivity in the pore fluid, IP is strongly affected by processes at the fluid-grain interface. During IP-survey, both resistive and capacitive properties of the soil are measured. As a result of IP studies, at least theoretically, additional information about spatial variations in lithology and chemical composition of the grain surface can be determined. IP measurements are made in the field using a four-electrode circuit. Measurements can be made in the time or frequency domain. In the first case, the voltage drop over time is measured after the current is stopped (Fig. 7). The gradual (rather than abrupt) decrease in measured voltage is a complex function of the electrical charge polarization at the fluid-grain interface, and the conduction within the pore fluid and along the grain boundaries.

Seigel [45] defined the apparent chargeability (m_a) as equation (3):

$$m_a = \frac{V_s}{V_p}, \quad (3)$$

where V_s is the secondary voltage (voltage immediately after the current is shut off) and V_p is the primary voltage [42].

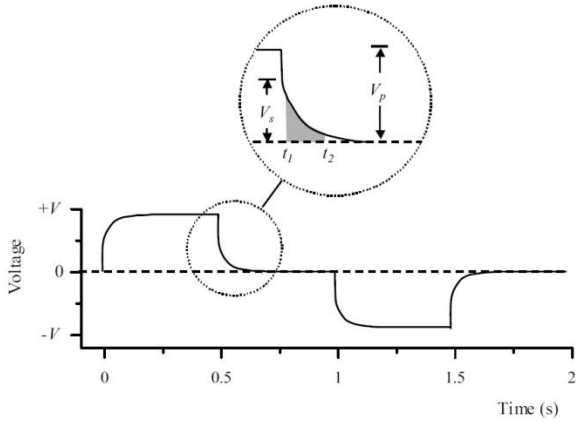

Fig. 7. *Measurement of time-domain induced polarization [42]*

Fig. 7. *Измерение поляризации, вызванной во временной области [42]*

In frequency-domain mode, a phase-shifted voltage relative to an injected alternating current is measured. Traditionally, the percent frequency effect (PFE) has been used as an IP measure in the frequency domain. Here, a comparison of impedance magnitudes is made at different injection frequencies. Alternatively, the impedance (in terms of magnitude and phase angle) may be used as a measure of IP. This is commonly referred to as complex resistivity. When the injected current is applied at different injection frequencies, an impedance spectrum is obtained. This is commonly referred to as spectral IP (SIP). IP can be measured in the field using a similar approach to that for DC resistivity. The potential electrodes should, ideally, be nonpolarizing (for example, copper-copper sulfate), although conventional DC resistivity electrodes were used with some success. To avoid electromagnetic coupling effects, the cable used for current injection should be short and isolated, as much as

possible, from cables connected to the potential electrodes. Dipole-dipole arrays for ground-surface surveys are often preferred because of their minimal coupling effects and safer operating conditions (particularly for long survey transects). For IP surveys, injection currents often need to be much higher than those used for DC resistivity to ensure good signal-to-noise ratios. This is particularly important when using a dipole-dipole electrode configuration [42].

Processing and interpreting resistivity and IP data

There are several methods for processing and interpreting resistivity and IP data. In the past, most interpretations were made based on electrical resistivity and apparent IP [46]. With the advancement of computer science and numerical analysis of inversion, it is now possible to directly investigate resistive and IP data. The Res2DInv software package is used to conduct dipole-dipole studies [47].

Pseudo-sectional drawing method

In most 2D resistances and IP surveys, pseudo-dimensional drawings are used. In this method, the mid-point of the electrodes that are measured is considered as a reading point. The vertical position of the reading value is located below the reading point, which is proportional to the distance of the electrodes. For IP surveys, the conventional method is the two-line cross-section, which converges at an angle of 45°.

From pseudo-sectional drawings, an approximate image of the distribution of resistances or subsurface IP is obtained. The conventional method of taking IP is dipole-dipole. This approach is widely used in IP operations due to the low efficiency of coupling between current and potential electrodes. In a model, several parameters change, which causes a change in the response of the model. In an inversion, we try to obtain the physical quantities that have the closest conditions to the real model.

Inversion of two-dimensional Resistivity and IP data

Data is controlled in terms of quality before inversion. In this process, noises created systematically or accidentally should be removed from the data. The issue of the absence of a unified model in the modeling of geophysical data is well-known. Data inversion uses different information to limit possible models. For example, in many surveys, there is information on subsurface geology that can contribute to the initial model. In an inversion, we always look for a model that meets the real conditions governing the environment [48, 49]. In all of the inversion methods, the initial model alternates so that the difference between the response of the model [50] and the actual data is minimized [51].

Results and discussion

Inverse Models of Resistivity and IP Data

Profile 1

This profile includes the dipole-dipole array with the parameters AB=MN=10 m, jump=10 m and up to eight jumps for MN were taken. Fig. 8 shows the induced polarization and resistivity model along with profile 1. On the resistivity model of this profile, there are generally three northern, central, and southern parts. The central part of the station, –60 to –10, at which the level is low, increases the resistance and then the resistance is reduced, which is probably related to the crushed zone. The southern part shown a higher resistance from station –60 to the south. The northern part of the point –10 to the north end has a high resistance and probably corresponds to the basaltic and andesitic sections. On the map of the induced polarization model of this profile, it can be seen that the central part mentioned above, which has less resistance, has less polarization as well. In the south, the amount of polarity rose, but at the same time, the amount of special resistance increased, which does not show sulfide mineralization, but also does not affect the surface of the earth. The surface rocks observed in this part are agglomerate rocks. In the north, there is a limestone rock that does not cross directly through the profile that intercepts the valley. The effects of mineralization on the ground also indicate the presence of mineralization at the station of zero to 10. Thus, on this profile, the range between the northern station 5 is to be examined up to a depth of 20 meters with a 20-degree angle, and a station 30 for a borehole with the depth of 40 meters, and angle of 25 degrees along with the profile and both to the south.

Profile 2

This profile includes the dipole-dipole array with the parameters AB=MN=20 m, jump=20 m and up to six jumps for MN were taken. As it is shown in Fig. 9, on the map, the resistance model of this profile separates the yellow-brown to read sections of the high-resistivity sections. Green and blue sections show lower relative resistivity. There is significant contact between station zero to –20. Limestones also have little effect on this profile. The resistivity amount at the ground level from station –20 to the south is generally high and at a depth of 20 meters in the same range were reduced. Due to the increase in the amount of polarity in the same range, geophysically, it is a suitable area for the presence of sulfide minerals, but there is no mineralization on the earth. On the other hand, in the north, the amount of resistance on the ground was reduced, which is natural due to the presence of alluvium, and then in-depth the amount of resistance increased, which increases the probability of the presence of the basic mass in this section. On the map of induction polarization, the generally visible boundaries on the earth's surface near the zero point of the profile where the effects of copper minerals such as malachite are observed have a low polarity density with a high green color, which does not show many extensions. It might be possible to link the anomaly between the station to zero and 20 with an anomaly in-depth, between stations 30 and 80. In this case, station 60 is suitable for drilling 20 degrees to the south along the profile to a depth of 50 meters. Station 60 is also proposed vertically up to 40 meters in depth to be drilled at a later stage.

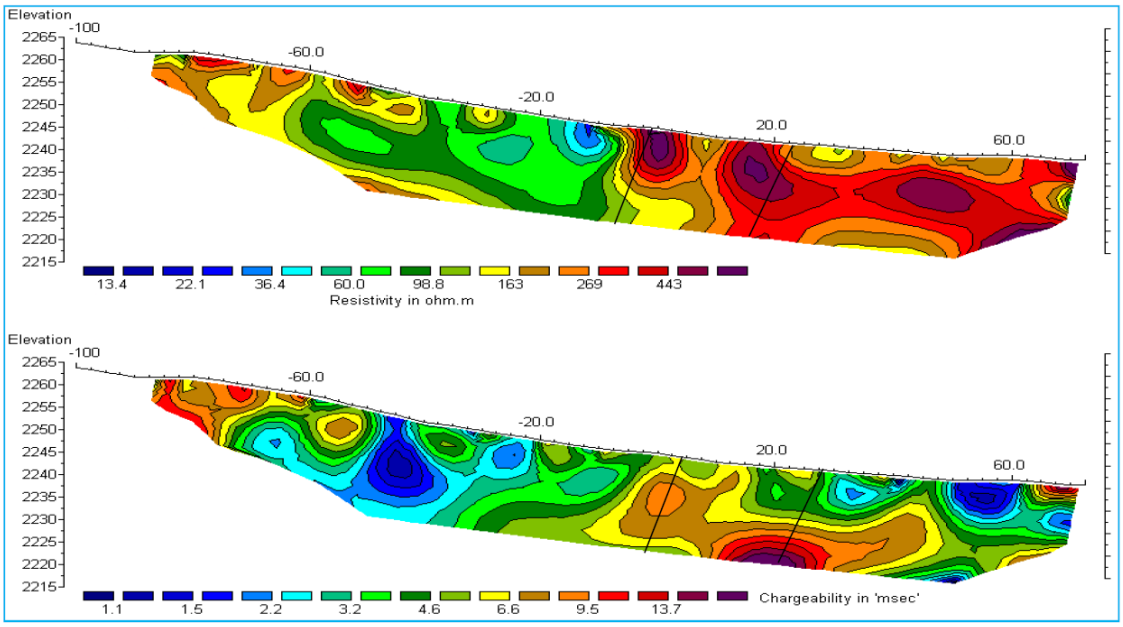

Fig. 8. *Up-resistivity and down-induced polarization model on profile 1*

Fig. 8. *Модель повышения удельного сопротивления и пониженной поляризации в профиле 1 с вынесенными проектными скважинами*

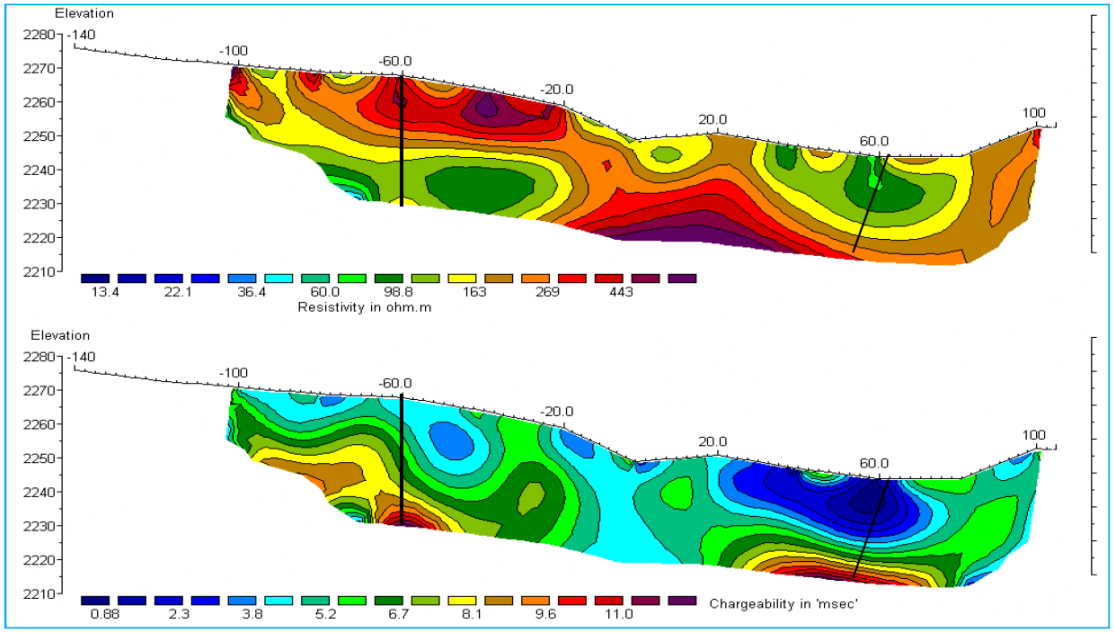

Fig. 9. *Up-resistivity and down-induced polarization model on profile 2*

Fig. 9. *Модель повышения удельного сопротивления и пониженной поляризации в профиле 2 с вынесенными проектными скважинами*

Profile 3

This profile includes the dipole-dipole array with the parameters AB=MN=20 m, jump=20 m and up to six jumps for MN were taken. On the map of the resistivity model in Fig. 10, high resistivity sections can be found, between stations –15 to 10, and also between stations 20 to 45 and from station 60 to the north, among these sections, resistance was reduced. The contacts or faults can be separated around stations number 50 and –15. On the section of the induced polarization model of this profile, superficial mineralizations can be found between stations 50 to 60, 30 to 40, 0 to 20, –10 to –20. More important than the superficial mineralizations, on this profile, significant anomalies, from the station 40 north to –20 in the south, from the depth of 10 to a depth of 40 meters extended. In this way, on this profile, station 30 and station 10 for drilling to 40 meters depth with a 20-degree angle to the south along the profile is suggested.

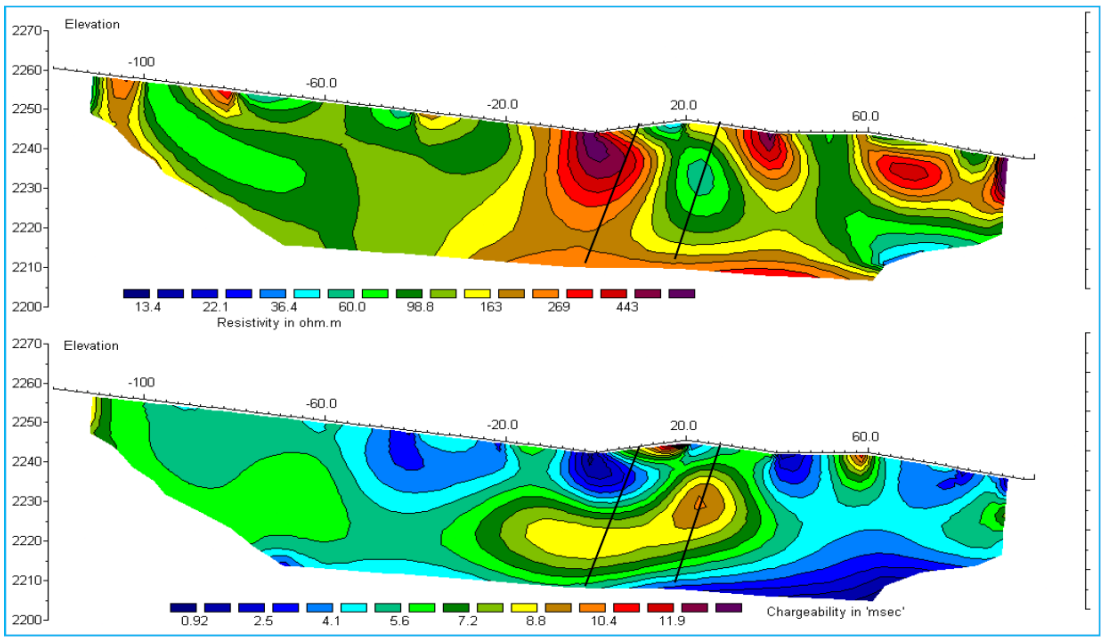

Fig. 10. *Up-resistivity and down-induced polarization model on profile 3*

Fig. 10. *Модель повышения удельного сопротивления и пониженной поляризации в профиле 3 с вынесенными проектными скважинами*

Profile 4

This profile includes the dipole-dipole array with the parameters AB=MN=20 m, jump=20 m and up to six jumps for MN were taken. Fig. 11 shows the model of resistivity and induced polarization of profile 4. On the map of the resistivity model, contacts can be seen at stations 60 and –90. At station –90 to the south, there are the agglomerate rocks. A low resistive part is seen between stations 15 to 45 in widths of 30 m. At station –80, it is also seen, in addition to low resistance, that the other part, located mainly on andesites and basalts, with depths from 10 to 15 m, starts from station 15 in the north, and some surface fragments go to station –70 in the south. On the map of the induced polarization model, in the southern part, the agglomerates show high polarity. The largest anomaly in terms of severity and extent is seen between stations –40 and –15. On this profile, the zero station is recommended for drilling up to a depth of 40 m with an angle of 25 degrees along with the profile to the south.

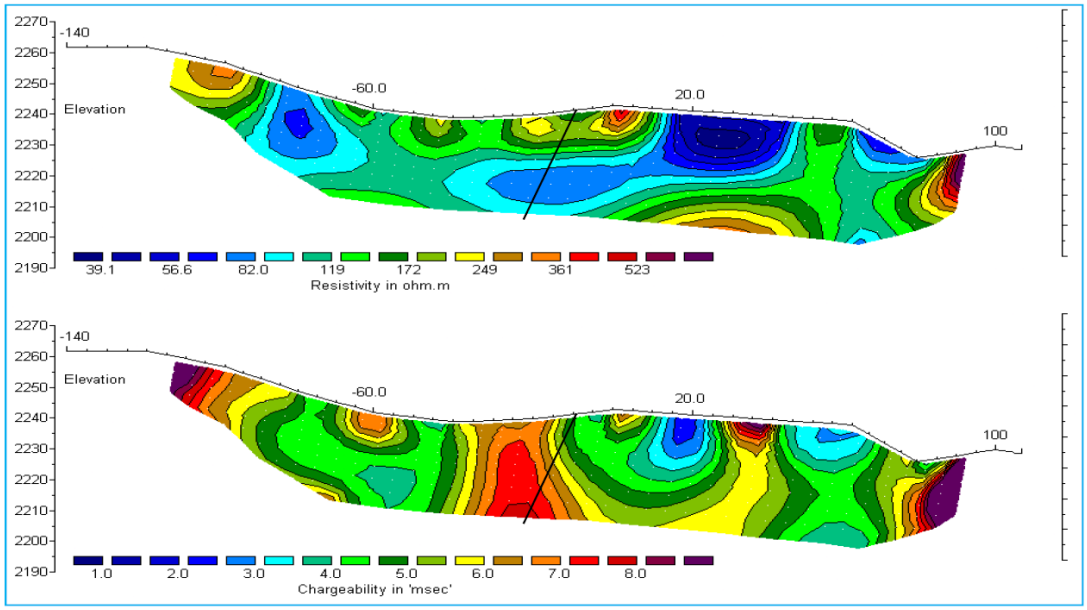

Fig. 11. *Up-resistivity and down-induced polarization model on profile 4*

Fig. 11. *Модель повышения удельного сопротивления и пониженной поляризации в профиле 4 с вынесенными проектными скважинами*

Profile 5

This profile includes the dipole-dipole array with the parameters AB=MN=20 m, jump=20 m and up to six jumps for MN were taken. As it is shown in Fig. 12, on the map, the resistivity profile model of this profile can be generally referred to as a central high strength section from the station 30 to 60 – to a width of approximately 90 ms on this profile, which is roughly spread vertically to the depth. This part corresponds to andesitic rocks containing mineralization. The amount of resistance was reduced to both sides of the south and north, which is likely to coincide with the alluvium because the amount of induced polarization was reduced as well. Of course, the presence of limestone in the northern part, on the surface, rose the resistance between stations 40 to 90 with a slight rupture. On the map of the induced polarization the model of this profile is referred to three areas that are characterized by three proposed lines for drilling. Although superficial mineralization is observed at a distance between stations –10 to –20 in the south and 10 to 20 in the north, the main anomalies are below the station's numbers –60, –20 and 20. In this way, on this profile, station 30 for drilling with the angle of 20 degrees to the south along the profile up to a depth of 40 m, and station –10 for drilling with the angle of 25 degrees to the south to a depth of 30 m and station –65 with the angle of 20 degrees to the north along with the profile up to a depth of 40 m on this profile are suggested.

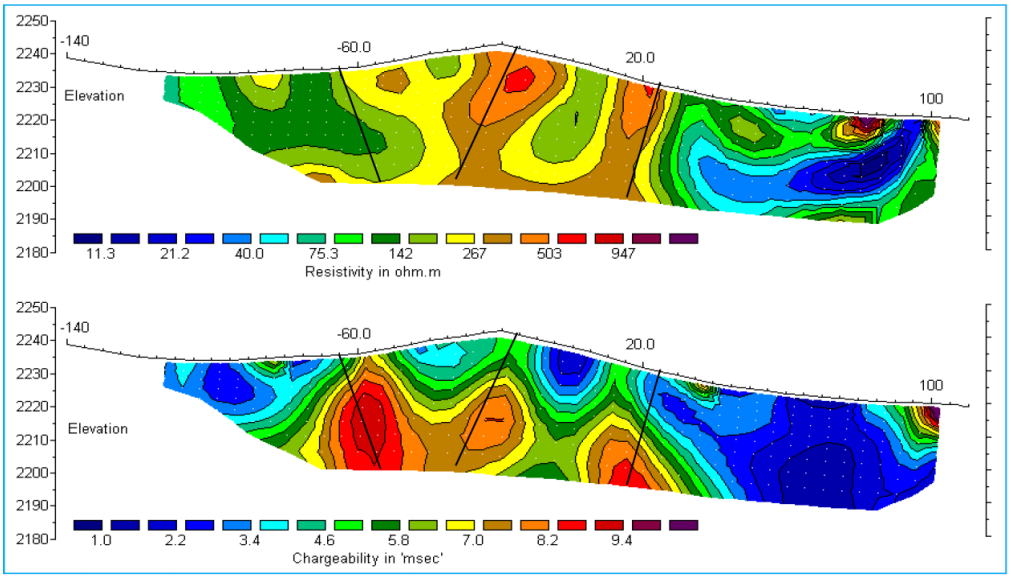

Fig. 12. *Up-resistivity and down-induced polarization model on profile 5*

Fig. 12. *Модель повышения удельного сопротивления и пониженной поляризации в профиле 5 с вынесенными проектными скважинами*

Conclusion

In general, four types of anomalies were identified in this investigation, which to some extent revealed the association of anomalies with the types of rocks and mineralization of the study area:

- The average value of the geophysical anomaly threshold is 250 ohm-m for resistivity and 7 mV/V for chargeability. This threshold was determined based on the geological and lithological characteristics of the target copper mineralization. In these values, the detection of copper mineralization is more likely than in others.
- Anomalies with low electrical resistivity, as well as low polarity, often correspond to quaternary alluvial deposits.
- Abnormalities with high electrical resistance, and low polarity, are consistent with limestones and are often superficial.
- Anomalies with high polarity and high resistance in the south of the profiles form altitude and correspond to the agglomerates.
- Anomalies with high polarity and higher relative resistance are associated with igneous masses, which are often composed of rocks of basaltic composition with ore mineralization. In cases where electrical resistance in this part of the rock is further reduced, it can be used to form the sulfide mass in this rock or to the extent of its contact with limestone.

Based on the position of the identified anomalies in each profile, the optimal location of the drills was determined. The proposed exact location of each drill is shown on the drawn cross-section of the profile.

REFERENCES

1. Khakmardan S., Shirazi A., Shirazy A., Hosseingholi H. Copper oxide ore leaching ability and cementation behavior, mesgaran deposit in Iran. *Open Journal of Geology*, 2018, vol. 09, no. 8, pp. 841–858.
2. Segura-Salazar J., Tavares L.M. Sustainability in the minerals industry: seeking a consensus on its meaning. *Sustainability*, 2018, vol. 10, no. 5, pp. 1–38.
3. Pokhrel L.R., Dubey B. Global scenarios of metal mining, environmental repercussions, public policies, and sustainability: a re-

view. *Critical Reviews in Environmental Science and Technology*, 2013, vol. 43, no. 21, pp. 2352–2388.
4. Campbell J.B., Wynne R.H. *Introduction to remote sensing*. 5th ed. Eds. J.B. Campbell, R.H. Wynne. New York, The Guilford Press, 2011. 662 p.
5. Ali S.H., Giurco D., Arndt N., Nickless E., Brown G., Demetriades A., Durrheim R., Enriquez M.A., Kinnaird J., Littleboy A., Meinert L.D., Oberhänsli R., Salem J., Schodde R., Schneider G., Vidal O., Yakovleva N. Mineral supply for sustainable development requires resource governance. *Nature*, 2017, vol. 543, no. 7645, pp. 367–372.
6. Sabins F.F. *Remote sensing-principles and interpretation*. New York, WH Freeman and company, 1987. 449 p.
7. Rahimdel M.J., Noferesti H. Investment preferences of Iran's mineral extraction sector with a focus on the productivity of the energy consumption, water and labor force. *Resour Policy*, 2020, vol. 67, pp. 1–15.
8. Alahgholi S., Shirazy A., Shirazi A. Geostatistical studies and anomalous elements detection, Bardaskan Area, Iran. *Open Journal of Geology*, 2018, vol. 8, no. 7, pp. 697–710.
9. Sabins F.F. Remote sensing for mineral exploration. *Ore Geology Reviews*, 1999, vol. 14, pp. 157–183.
10. Timkin T., Voroshilov V., Yanchenko O., Suslov J., Korotchenko T. Geology, geochemistry and gold-ore potential assessment within Akimov ore-bearing zone (the Altai Territory). *IOP Conference Series: Earth and Environmental Science*, 2016, vol. 43, pp. 1–5.
11. Shirazi A., Shirazy A., Karami J. Remote sensing to identify copper alterations and promising regions, Sarbishe, South Khorasan, Iran. *International Journal of Geology and Earth Sciences*, 2018, vol. 4, no. 2, pp. 36–52.
12. Pshenichkin A., Timkin T., Oskina Y. Noble metals in rocks and ores of Maysko-Lebed ore field (Mountain Shoriya). *IOP Conference Series: Earth and Environmental Science*, 2015, vol. 24, pp. 1–6.
13. Shirazi A., Shirazy A., Saki S., Hezarkhani A. Introducing a software for innovative neuro-fuzzy clustering method named NFCMR. *Global Journal of Computer Sciences: theory and research*, 2018, vol. 8, no. 2, pp. 62–69.
14. Gupta R.P. *Remote sensing geology*. Springer, 2017. 428 p.
15. Shirmard H., Farahbakhsh E., Müller R.D., Chandra R. A review of machine learning in processing remote sensing data for mineral exploration. *Remote Sensing of Environment*, 2022, vol. 268, pp. 1–21.
16. Pour A.B., Hashim M., Hong J.K., Park Y. Lithological and alteration mineral mapping in poorly exposed lithologies using Landsat-8 and ASTER satellite data: north-eastern Graham Land, Antarctic Peninsula. *Ore Geology Reviews*, vol. 108, pp. 112–133.
17. Mahanta P., Maiti S. Regional scale demarcation of alteration zone using ASTER imageries in South Purulia Shear Zone, East India: implication for mineral exploration in vegetated regions. *Ore Geology Reviews*, 2018, vol. 102, pp. 846–861.
18. Sonbul A.R., El-Shafei M.K., Bishta A.Z. Using remote sensing techniques and field-based structural analysis to explore new gold and associated mineral sites around Al-Hajar mine, Asir terrane, Arabian Shield. *Journal of African Earth Sciences*, 2016, vol. 117, pp. 285–302.
19. Shirazy A., Ziaii M., Hezarkhani A., Timkin T.V., Voroshilov V.G. Geochemical behavior investigation based on K-means and artificial neural network prediction for titanium and zinc, Kivi region, Iran. *Bulletin of the Tomsk Polytechnic University. Geo Assets Engineering*, 2021, vol. 332, no. 3, pp. 113–125. In Rus.
20. Woźniak S.B., Stramski D. Modeling the optical properties of mineral particles suspended in seawater and their influence on ocean reflectance and chlorophyll estimation from remote sensing algorithms. *Applied Optics*, 2004, vol. 43, no. 17, pp. 3489–3503.
21. Dowling R., Newsome D. Geotourism's issues and challenges. *Geotourism*, 2006, pp. 242–254.
22. Mehdipour Ghazi J., Hamdollahi M., Moazzen M. Geotourism of mining sites in Iran: an opportunity for sustainable rural development. *International Journal of Geoheritage and Parks*, 2021, vol. 1, no.9, pp. 129–142.
23. Shirazy A., Hezarkhani A., Timkin T., Shirazi A. Investigation of magneto-/radio-metric behavior in order to identify an estimator model using K-means clustering and Artificial Neural Network (ANN) (Iron Ore Deposit, Yazd, IRAN). *Minerals*, 2021, vol. 11, no. 12, pp. 1–18.
24. Mohammadi N.M., Hezarkhani A., Maghsoudi A. Application of K-means and PCA approaches to estimation of gold grade in Khooni district (central Iran). *Acta Geochimica*, 2018, vol. 37, pp. 102–112.
25. Liu Y., Zhou K., Cheng Q. A new method for geochemical anomaly separation based on the distribution patterns of singularity indices. *Computers & Geosciences*, 2017, vol. 105, pp. 139–147.
26. Shirazy A., Ziaii M., Hezarkhani A., Timkin T. Geostatistical and remote sensing studies to identify high metallogenic potential regions in the Kivi Area of Iran. *Minerals*, 2020, vol. 10, pp. 1–25.
27. Azizi H., Tarverdi M. A., Akbarpour A. Extraction of hydrothermal alterations from ASTER SWIR data from east Zanjan, northern Iran. *Advances in Space Research*, 2010, vol. 46, no. 1, pp. 99–109.
28. Veeken P.C.H., Legeydo P.J., Davidenko Y.A., Kudryavceva E.O., Ivanov S.A., Chuvaev A. Benefits of the induced polarization geoelectric method to hydrocarbon exploration. *Geophysics*, 2009, vol. 74, no. 2, pp. 1MA-Z35.
29. Yuval D., Oldenburg W. DC resistivity and IP methods in acid mine drainage problems: results from the Copper Cliff mine tailings impoundments. *Journal of Applied Geophysics*, 1996, vol. 34, no. 3, pp. 187–198.
30. Ward S.H. Resistivity and induced polarization methods. Geotechnical and environmental geophysics: Vol. I. *Review and Tutorial, Investigations in Geophysics. Society of Exploration Geophysicists*, 1990, pp. 147–190.
31. Karimpour M., Stern C., Farmer L., Saadat S. Review of age, Rb-Sr geochemistry and petrogenesis of Jurassic to Quaternary igneous rocks in Lut Block, Eastern Iran. *Geopersia*, 2011, vol. 1 (1), pp. 19–54.
32. Richards J.P., Spell T., Rameh E., Razique A., Fletcher T. High Sr/Y magmas reflect arc maturity, high magmatic water content, and porphyry Cu ± Mo ± Au potential: examples from the Tethyan Arcs of Central and Eastern Iran and Western Pakistan. *Economic Geology*, 2012, vol. 107 (2), pp. 295–332.
33. Pang K.N., Chung S.L., Zarrinkoub M.H., Khatib M.M., Mohammadi S.S., Chiu H.Y., Chu C.H., Lee H.Y., Lo C.H. Eocene–Oligocene post-collisional magmatism in the Lut–Sistan region, eastern Iran: magma genesis and tectonic implications. *Lithos*, 2013, vol. 180 (181), pp. 234–251.
34. Etemadi A., Nadermezerji S., Karimpour M.H., Malekzadeh Shafaroudi A., Santos J.F., Ribeiro S. Geochemistry, petrogenesis, zircon UPb geochronology and SrNd isotopic composition of Kuh-e-Shah volcanic rocks: implications for an active continental margin along with eastern Iran during the Paleogene. *Lithos*, 2020, vol. 378 (379), pp. 105778.
35. Nagy Z. Advances in the combined interpretation of seismics with magnetotellurics1. *Geophysical Prospecting*, 1996, vol. 44 (6), pp. 1041–1083.
36. Zhuang Z., Jian-ming L., Chang-ming Y., Qing-dong Z., Ya-jun B., Ai-guo Q., Mo N., Zhuang Z., Jian-ming L., Chang-ming Y., Qing-dong Z., Ya-jun B., Ai-guo Q., Mo N. Application of integrated geophysical prospecting methods in the evaluation of BIF deposits-a case study in Inner Mongolia aohanqi sijiazi BIF deposits. *Progress in Geophysics*, 2013, vol. 28 (4), pp. 2078–2084.
37. An Z., Di Q. Investigation of geological structures with a view to HLRW disposal, as revealed through 3D inversion of aeromagnetic and gravity data and the results of CSAMT exploration. *Journal of Applied Geophysics*, 2016, vol. 135, pp. 204–211.
38. Zarjabad H.H., Zareie A., Harchegani T.B., Farjami M. Archaeological investigation of metal smelting in Eastern Iran. Case study. Mesgaran Area one of the most ancient metal smelting plants in South Khorasan. *International journal of review in life sciences*, 2015, vol. 8, no. 5, pp. 1092–1104.
39. Ghorbani M. *A summary of geology of Iran*. Dordrecht, The Netherlands, Springer, 2013. pp. 45–64.
40. Mohammadi S.S., Vosoughi A.M., Pourmoafi S.M., Emami M.H., Khatib M.M. Petrography, geochemistry, genesis and tectonic setting of Mesgaran Area Granitoids (South-East of Birjand). *Journal of sciences*, 2007, vol. 17, no. 65, pp. 1–15.
41. Agharezaei M., Hezarkhani A. Delineation of geochemical anomalies based on Cu by the boxplot as an exploratory data analysis (EDA) method and concentration-volume (CV) fractal modeling in Mesgaran mining area, Eastern Iran. *Open Journal of Geology*, 2016, vol. 6, no. 10, pp. 1269–1278.

42. Binley A., Kemna A. DC resistivity and induced polarization methods. *Hydrogeophysics*, 2005, pp. 129–156.
43. Fink J.B., McAlister E.O., Sternberg B.K., Wieduwilt W.G., Ward S.H. *Induced polarization, applications and case histories*. Vol. 4. Tulsa, Oklahoma, Investigations in geophysics, society of exploration geophysicists, 1990. 411 p.
44. Campbell D.L., Fitterman D.V. Geoelectrical methods for investigating mine dumps. *ICARD 2000. Proc. of the 5th International Conference on Acid Rock Drainage, Society for Mining, Metallurgy and Exploration*. Inc., Littleton, Colorado, 2000. pp. 1513–1523.
45. Seigel H.O. Mathematical formulation and type curves for induced polarization. *Geophysics*, 1959, vol. 24, no. 3, pp. 547–565.
46. White R.M.S., Collins S., Loke M.H. Resistivity and IP arrays, optimised for data collection and inversion. *Exploration Geophysics*, 2003, vol. 34, no. 4, pp. 229–232.
47. Olayinka A.I., Yaramanci U. Assessment of the reliability of 2D inversion of apparent resistivity data. *Geophysical Prospecting*, 2000, vol. 48, no. 2, pp. 293–316.
48. Dahlin T., Rosqvist H., Leroux V. Resistivity-IP for landfill applications. *First Break*, 2010, vol. 28, no. 8, pp. 101–105.
49. Loke M.H, Lane J.W.Jr. Inversion of data from electrical resistivity imaging surveys in water-covered areas. *Exploration Geophysics*, 2004, vol. 35, no. 4, pp. 266–271.
50. Loke M.H., Acworth I., Dahlin T. A comparison of smooth and blocky inversion methods in 2D electrical imaging surveys. *Exploration Geophysics*, 2003, vol. 34, no. 3, pp. 182–187.
51. Khosravi V., Shirazi A., Shirazy A., Hezarkhani A., Pour A.B. Hybrid Fuzzy-Analytic Hierarchy Process (AHP) model for porphyry copper prospecting in Simorgh Area, Eastern Lut Block of Iran. *Mining*, 2022, vol. 2, no. 1, pp. 1–12.

Received: 2 March 2022.

Information about the authors

Adel Shirazy, PhD, assistant, Amirkabir University of Technology (Tehran Polytechnic).
Ardeshir Hezarkhani, PhD, full professor, Amirkabir University of Technology (Tehran Polytechnic).
Aref Shirazi, PhD, assistant, Amirkabir University of Technology (Tehran Polytechnic).
Timofey V. Timkin, Cand. Sc., associate professor, National Research Tomsk Polytechnic University.
Valery G. Voroshilov, Dr. Sc., professor, National Research Tomsk Polytechnic University.

УДК 550.8+550.84.09

ПРИМЕНЕНИЕ ГЕОФИЗИЧЕСКИХ МЕТОДОВ УДЕЛЬНОГО ЭЛЕКТРИЧЕСКОГО СОПРОТИВЛЕНИЯ И ВЫЗВАННОЙ ПОЛЯРИЗАЦИИ ПРИ ПОИСКЕ МЕДНЫХ РУД, ЮЖНЫЙ ХОРАСАН, ИРАН

Адель Ширази[1],
Adel.shirazy@shahroodut.ac.ir

Ардешир Хезархани[1],
Ardehez@aut.ac.ir

Ареф Ширази[1],
Adel.shirazy@shahroodut.ac.ir

Тимкин Тимофей Васильевич[2],
timkin@tpu.ru

Ворошилов Валерий Гаврилович[2],
v_g_v@tpu.ru

[1] Технологический университет им. Амир Кабира (Тегеранский политехнический институт), Иран, 1591634311, Тегеран, Авеню Хафеза.

[2] Национальный исследовательский Томский политехнический университет, Россия, 634050, г. Томск, пр. Ленина, 30.

Актуальность. *Это первые геофизические исследования на перспективной площади Месгаран. На основе ранее проведенных общих геологических исследований в районе обнаружены проявления медной минерализация. Геолого-промышленный тип в этой области был определен как вулканогенно-колчеданный в офиолитовых комплексах (кипрский тип). Сложность геологического строения определяет необходимость применения геофизических методов исследования и прогнозирования для планирования горно-буровых работ.*

Основной целью *данного исследования является применение геофизических методов при поиске месторождений полезных ископаемых, моделировании геологической среды, прогнозировании новых рудоносных площадей, перспективных участков и проектировании горных выработок.*

Объект: *район Месгаран, провинция Южный Хорасан, Иран.*

Методы. *Для получения дополнительной информации о недрах использовались геофизические методы удельного электрического сопротивления (Rs) и вызванной поляризации (IP). Для геоэлектрических съёмок были запроектированы и реализованы пять профилей, по которым было снято 784 точки замера. Профили ориентированы в широтном и меридиональном направлениях вдоль зон минерализации. Диполь-дипольная решетка спроектирована с параметрами AB=MN=20 м, шагом=20 м и до 6 шагов для MN.*

Результаты. *Было выявлено четыре типа аномалий, что позволило сделать геофизическую интерпретацию связи их с типами пород и оруденением на изучаемой территории: 1) аномалии с низким электрическим сопротивлением, а также низкой поляризуемостью часто соответствуют четвертичным аллювиальным отложениям; 2) аномалии с высоким электрическим сопротивлением и низкой поляризуемостью характерны для осадочных отложений; 3) аномалии с высокой поляризуемостью и высоким сопротивлением соответствуют рыхлым пеплово-шлаковым агломератам вулканического происхождения; 4) аномалии с высокой поляризуемостью и более высоким относительным сопротивлением связаны с массивами вулканических пород, представленных обычно андезибазальтами. По положению выявленных на 5 профилях аномалий определено оптимальное расположение буровых скважин.*

Ключевые слова:
Удельное электрическое сопротивление, вызванная поляризация, месторождение меди, геофизическая модель, район Месгаран, Иран.

Информация об авторах

Ширази Ад., PhD, ассистент Технологического университета им. Амир Кабира (Тегеранский политехнический институт).

Хезархани А., PhD, професор Технологического университета им. Амир Кабира (Тегеранский политехнический институт).

Ширази Ар., PhD, ассистент Технологического университета им. Амир Кабира (Тегеранский политехнический институт).

Тимкин Т.В., кандидат геолого-минералогических наук, доцент отделения геологии Инженерной школы природных ресурсов Национального исследовательского Томского политехнического университета.

Ворошилов В.Г., доктор геолого-минералогических наук, профессор отделения геологии Инженерной школы природных ресурсов Национального исследовательского Томского политехнического университета.

Поступила 02.03.2022 г.